Institute of Sound
and Vibration Research

Determination of the Vibration and Acoustic Radiation of a Concrete Railway Sleeper

C. Bosquet, N.S. Ferguson and D.J. Thompson

ISVR Technical Memorandum 827

December 1997

University
of Southampton

SCIENTIFIC PUBLICATIONS BY THE ISVR

Technical Reports are published to promote timely dissemination of research results by ISVR personnel. This medium permits more detailed presentation than is usually acceptable for scientific journals. Responsibility for both the content and any opinions expressed rests entirely with the author(s).

Technical Memoranda are produced to enable the early or preliminary release of information by ISVR personnel where such release is deemed to the appropriate. Information contained in these memoranda may be incomplete, or form part of a continuing programme; this should be borne in mind when using or quoting from these documents.

Contract Reports are produced to record the results of scientific work carried out for sponsors, under contract. The ISVR treats these reports as confidential to sponsors and does not make them available for general circulation. Individual sponsors may, however, authorize subsequent release of the material.

UNIVERSITY OF SOUTHAMPTON

INSTITUTE OF SOUND AND VIBRATION RESEARCH

STRUCTURAL DYNAMICS GROUP

Determination of the Vibration and Acoustic Radiation of a Concrete Railway Sleeper

by

C. Bosquet, N.S. Ferguson and D.J. Thompson

ISVR Technical Memorandum No. 827

December 1997

Authorized for issue by
Dr R J Pinnington
Group Chairman

Preface

This memorandum forms the result of a project carried out by Cédric Bosquet in the summer of 1997. The author completed the M.Sc. in Sound and Vibration Studies as a visiting exchange student and as such was not obliged to complete a project as a thesis. He performed the project described here voluntarily in order to take full opportunity of his visit to the ISVR to widen his experience.

Unfortunately due to the need to return to France to complete his course in Lyon, the work has been left with some loose ends, but it has been decided to publish it in its current state so that the progress which has been made is at least recorded.

D.J. Thompson
N.S. Ferguson
(supervisors)

ACKNOWLEDGEMENTS

Many thanks to my supervisors, Dr. D. J. THOMPSON and Dr. N. FERGUSON, for their help and encouragement throughout the project.

Thanks to the structural dynamics group for letting me use their instrumentation. In particular, I would like to thank Richard Grice for helping me to get started with the analyser and for his helpful comments in ways of doing the experiment.

Thanks also to the technical staff for their availability and kindness. In particular, I would like to thank Mr. C. Chalk for always making sure that my sleeper was moved in time and at the right place.

Finally, thank to the Institute of Sound and Vibration Research for accepting me to follow the MSc course during this European exchange program with INSA de Lyon (Institut National des Sciences Appliquées de Lyon). Especially, I would like to thank Professor F. J. FAHY for organising my arrival here in the ISVR and for always advising me throughout the twelve months of my stay.

It was a great pleasure for me to spend one full year in the ISVR where I could follow a high quality and professional course and obtain great experience during the project as well as improve my level in English.

TABLE OF CONTENTS

1-INTRODUCTION

1.1 Description of the problem

The noise from trains is a major problem for the expansion of the railway network. In particular, controversy often arises from the proposed high-speed French TGV lines. Although the expansion of the high-speed French train is part of the modernisation of the country, major objections are raised on environmental grounds, and in particular due to the noise that would be generated by the trains.

This rolling noise from trains comes mainly from wheel/rail interactions that generate the vibrations of these two components. The wheel-rail rolling noise is generally attributed to structural vibrations of the wheels and rails, excited from the contact patch area. This contact patch area is the surface of contact between the wheels and the rail during the motion of the train. Indeed, the main excitation is caused by the wheel and rail roughness (undulations), which introduce a relative vibration between the wheel and the rail. See reference [1].

Previous research has led to the construction of mathematical models for the wheel and rail radiation to predict their relative contribution (see reference [2]), and then to the construction of models described in references [3] and [4], based respectively on the finite element and periodic structure method. These models have been included within the software package TWINS (references [1] and [5]). This Track-Wheel Interaction Noise Software package was developed for the C163 Expert Committee of the European Rail Research Institute (ERRI) and is intended as a tool with which different designs of wheel and track can be assessed in terms of their noise generation. The figure 1 shows an overview of these TWINS models.

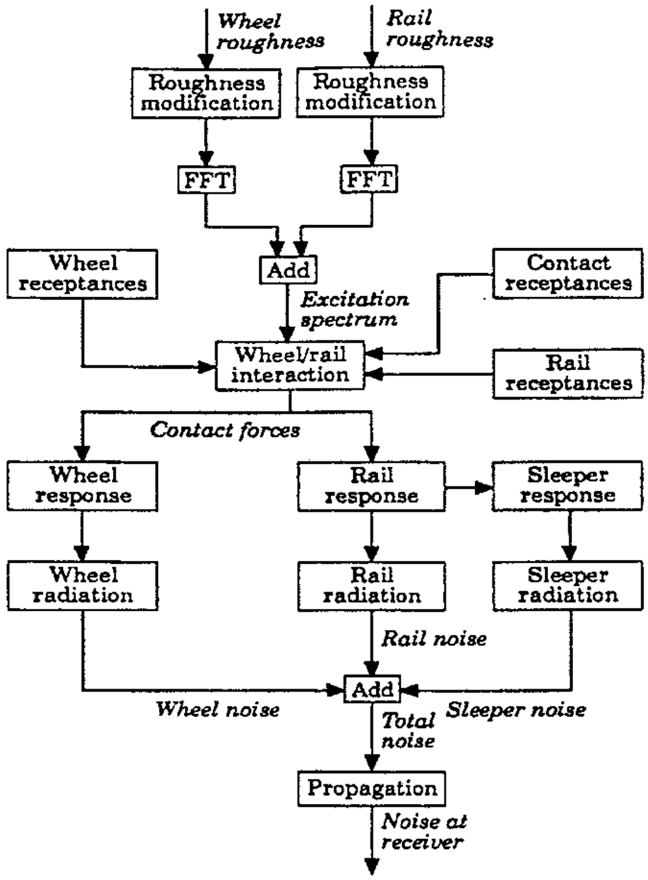

Figure 1 : An overview of the TWINS model for rolling noise

Although the radiation and vibration of the wheel and the rail have been modelled with a lot of improvement for a number of years, the radiation from the sleepers (pieces of wood or concrete that support the rail) has only been recently considered in the models, see references [6] and [7], and has not yet been validated. Besides, the possible radiation from the ballast (stone chippings on which the track is laid) has been ignored up till now.

In order to know the contribution of each component to the rolling noise, we need to study the theoretical models of these components. Although, in this project we are more interested in the sleeper vibrations and noise radiation, it is nevertheless essential to understand the dynamics of the other components such as the wheel and the rail.

1.2 Background knowledge

1.2.1 noise radiation

Early studies by Thompson [2] considered the mathematical models of the radiation from each component (wheel and rail), from which the relative contributions could easily be seen. These models were constructed because the current measurement techniques were inadequate to resolve this. Reference [2] also describes the results of applying these models to experimental data.

It could be seen that the prediction and measurement were in good agreement for all the conditions of the experiment between 630 Hz and 2500 Hz, and for most conditions over the full frequency range of the experiment of 250 Hz to 5000 Hz. From these models the relative importance of wheel and rail in producing the total radiated sound was established. They were both found to be important at and above 1250 Hz. Below this frequency the rail was the major radiator. Unfortunately, this paper does not explain in detail the models used to predict the sound radiated from the wheel and the rail, concentrating on the relative importance of the wheel and the rail in the rolling noise.

New models for the sound radiation from the wheel and the track, described in reference [1], have been implemented in TWINS. The sound power is calculated by combining predicted vibration spectra with radiation efficiencies in one-third octave bands. Results in [5] show once more the wheel to be dominant at high frequencies and the track at low frequencies. However unlike the earlier work, the sleeper is now shown to be important at frequencies up to 250-500 Hz, or for a wooden sleeper even 1 KHz. Different models of radiation are available for the wheel, the rail and the sleepers. Much more detail is given in [6] for these radiation models. It is important to note that the radiation from the vibration of the ballast is completely ignored.

The model of the radiation of the wheel is based on simple semi-analytical formulae for the radiation efficiency of various types of motion, knowing that three types of motion are distinguished : axial, radial and rotational (torsion of the wheel). Work is currently underway at the ISVR to improve this model, as part of the Silent Freight EU project.

The model of the rail radiation, described in [6] uses the principle of replacing a vibrating structure by series of fictitious elementary acoustic sources located inside the original structure boundary. The rail cross section is filled with a series of source triples, each made up of one monopole and two dipoles. The sleeper cross section is modelled similarly, except that it is defined only by a single quadrilateral whereas the rail cross section is divided into four quadrilaterals.

1.2.2 wheel vibration

Work by Thompson [3] on the model of wheel-rail interaction incorporates detailed predictions of the vibration properties of the wheel, which is a highly damped resonant structure. The use of a model of wheel vibration based on the finite element method, although not new in itself, represents a significant improvement on previous rolling noise models described in [8]. Experimental investigations have been carried out to measure the natural frequencies, mode shapes and damping ratios of various wheel types and reasonable agreement has been found with finite element predictions.

The free vibration of a wheel is also modelled in [1] by using finite elements. From the modal basis derived from this finite element analysis, the frequency response and the vibrational response of the wheel on the track are predicted in TWINS by using a modal summation. The model also includes the effects of wheel rotation.

1.2.3 rail vibration

While the wheel is a finite body, the rail is effectively infinite. It therefore acts as wave guide to structural waves which propagate away from the excitation point. At any given frequency, various different waves are permitted. At low frequency these are simple bending and torsional waves, but at higher frequencies the cross-section deforms allowing other wave types to propagate. Moreover, a rail has greater damping than a wheel, due to its supports (rail pad, sleepers and ballast) and this leads to a decay of the vibration with distance along the rail.

Unlike the wheel, the finite element method cannot be used directly to represent an infinite rail. However, it is possible to use periodic structure theory (see references [3] and [4]) to model an infinite beam-like structure such as a rail by considering it as a periodic structure of arbitrary periodic length. Finite element models can then be used to define the periodic element. The sleepers, railpad and ballast were also included, although only as equivalent continuous layer of mass/stiffness.

The receptance can be calculated from this periodic structure theory model by assembling the response at each frequency from the components of the various permissible waves. Finally predicted receptances were compared with published experimental results and good agreement was generally found.

Three alternative models, as described in [9], are available in TWINS for the track dynamics and are shown on figure 2 :

* Track model 1 : Continuously supported beam model.

The track is considered as a Timoshenko beam on a continuous support. The support consists of a resilient layer (the railpads), a mass layer (the sleepers) and a second resilient layer (the ballast). It is similar to the continuous model of Grassie [10], although the damping of the pads and ballast is modelled by hysteretic loss factor rather than viscous dampers.

* Track model 2 : Periodically supported beam model.
The second track model includes the periodic nature of the track. The support consists, as above, of spring-mass-spring systems, with hysteretically damped springs representing pad and ballast, and mass representing the sleeper.

* Track model 3 : Rail model including cross-section deformation developed in [3] and described above.

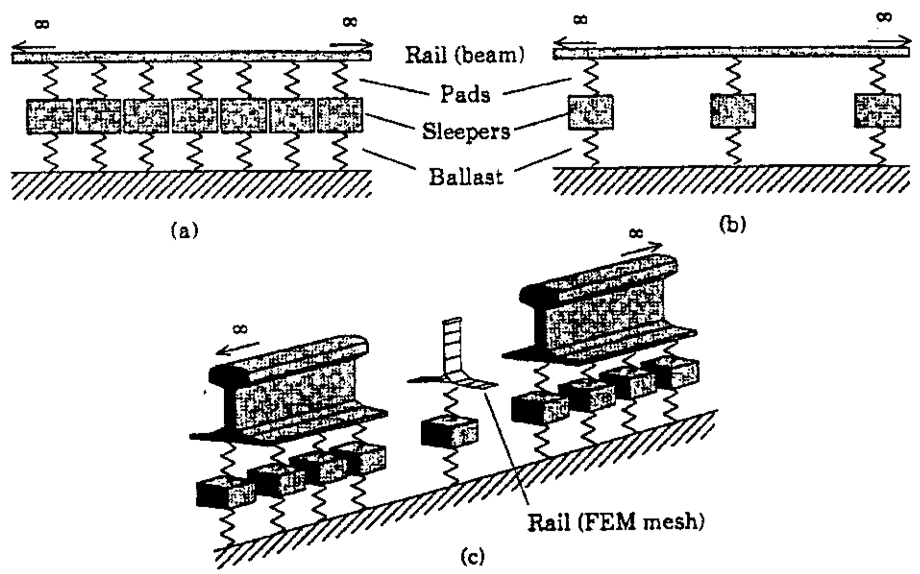

Figure 2 : Model for track vibration: (a) continuously supported beam; (b) periodically supported beam; (c) continuously supported rail model including cross-sectional deformation.

Experimental results obtained on several European tracks are presented in [11] and the validity of the models is assessed by means of comparisons between experiments and simulations : generally good agreement is found.

1.2.4 wheel-rail interaction

The interaction between wheel and rail is modelled introducing a relative displacement input between these two components due to the roughness on the wheel and rail surfaces. The model, described in [3], has been constructed to couple the wheel and the rail receptances, allowing six coupling co-ordinates. It is an improvement on earlier models by Remington [8] and that also used by Grassie [10].

The rolling noise is generated by surface irregularities ("roughness") on the wheel and/or rail running surface. Therefore, roughness needs to be measured and included in TWINS. The input data consists of the spatial data on a series of parallel lines across the contact patch. A model is included to calculate the average roughness input to the system from these data in the spatial domain. The details of the input roughness are given in [1].

The roughness induces a vertical relative displacement between the wheel and the rail or in the Hertzian contact spring, the motion of each depending on the relative amplitudes (and phase) of their receptances. Coupling in the lateral direction is represented by a creep force element. The model of this wheel-rail interaction is described in [1] and shown on figure 3.

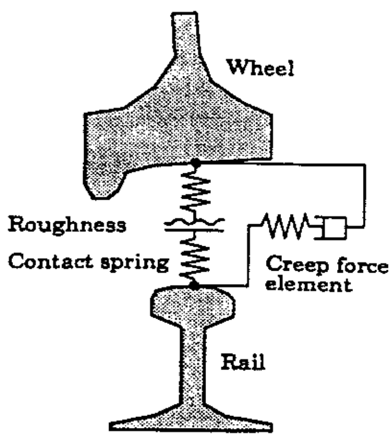

Figure 3 : Details of the wheel-rail interaction.

1.3 Reciprocity method

A number of the measurements presented in this report make use of the principle of reciprocity.

The basis of this method, described in [13], is the fundamental principle that the transfer function from a source at one point to a response at a second point is the same as the transfer function with the source and the response interchanged. Moreover it is essential to check that the system is linear and passive and that the product between input and output variable represents the power flow into the system due to that input, i.e. one pair might be a force and collinear velocity on a structure, or acoustic sound pressure and volume velocity. We would like to apply this method to the radiated sound from a vibrating solid surface.

The vibro-acoustic reciprocity technique is described in reference [14] and the principle is shown on figure 4. In particular, the transfer function from surface vibrating to radiated sound pressure is determined reciprocally using a monopole source at the receiver point and measuring the transfer function between its source strength and sound pressure on the surface of the non-vibrating body.

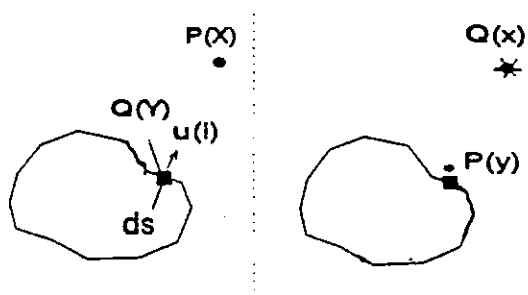

FIGURE 4 : Principle of a vibro-acoustic reciprocity.

$$\frac{p(X)}{Q(Y)} = \frac{p(X)}{u(i)ds} = \frac{p(Y)}{Q(X)} \qquad (1)$$

Measurements were performed according to the reciprocity principle, by placing a small, omni-directional and calibrated monopole source Q(X) at the receiver point and measuring the sound pressure $p(Y)_i$ on the sub-surface i of the nonrunning machine to obtain the acoustic transfer function. The pressure was measured by a microphone.

It has been demonstrated that it was not only possible to predict the sound pressure at a receiver point but it follows from the results that the relative contribution of the sub-components of a vibrating engine to the sound pressure may be determined as well. Indeed, the sound pressure is obtained by integrating the contribution of all the sub-areas. Therefore, it is clear that the contribution of one component can be found by integrating only the area of this component.
This is therefore quite interesting because it could be possible to try this technique on a track and determine at low frequency the relative contribution of the sleeper.

1.4 Description of the sleeper

The sleeper studied here is a re-inforced concrete design, manufactured by TARMAC. Its main dimensions are shown in figure 5.

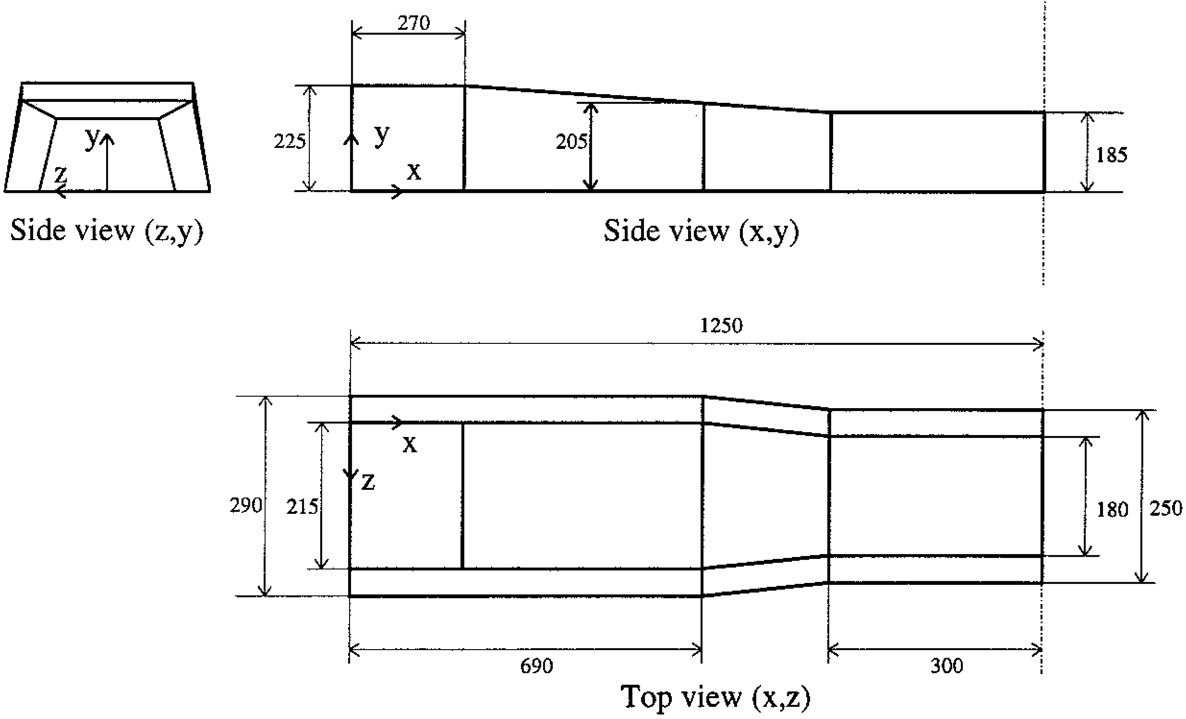

Figure 5 : half a sleeper showing dimensions

This sleeper is one of 56 supplied as part of a new test facility installed for the ISVR at the Chilworth Laboratories. In a subsequent phase of the work its vibration and acoustic properties will also be measured in situ. (It has been hoped to carry this out as part of the current project but late delivery of the test facility prevented this).

1.5 Work carried out

The work reported here consists of two experiments. In the first, described in chapter 2, a modal analysis is performed on the sleeper. In the second, described in chapter 3, the radiated sound power due to a unit force is determined reciprocally. Finally in chapter 4, the result are combined to derive the radiation efficiency of the sleeper.

2- MODAL ANALYSIS EXPERIMENT

2.1 Presentation of the experiment

The aim of this experiment is to excite the sleeper with an instrumented hammer to obtain the velocity distribution of the sleeper within a frequency range of 0-3200 Hz. Then, thanks to a modal analysis software, it is also possible to determine the natural frequencies, the mode shapes and the damping of the sleeper.

Then, in order to get the velocity distribution, the sleeper has to be meshed by dividing the structure into small areas delimited by points marked on the sleeper (node points). This mesh, once created on the structure, is re-created in the modal analysis software MESHGEN^{TM} from ICATS. The co-ordinates of the nodes are listed in Appendix A and the mesh is shown in figure 6. It has to be noted that only half of the sleeper is considered in the study because of the symmetry of the structure and the assumption that both sides of the sleeper behave identically.

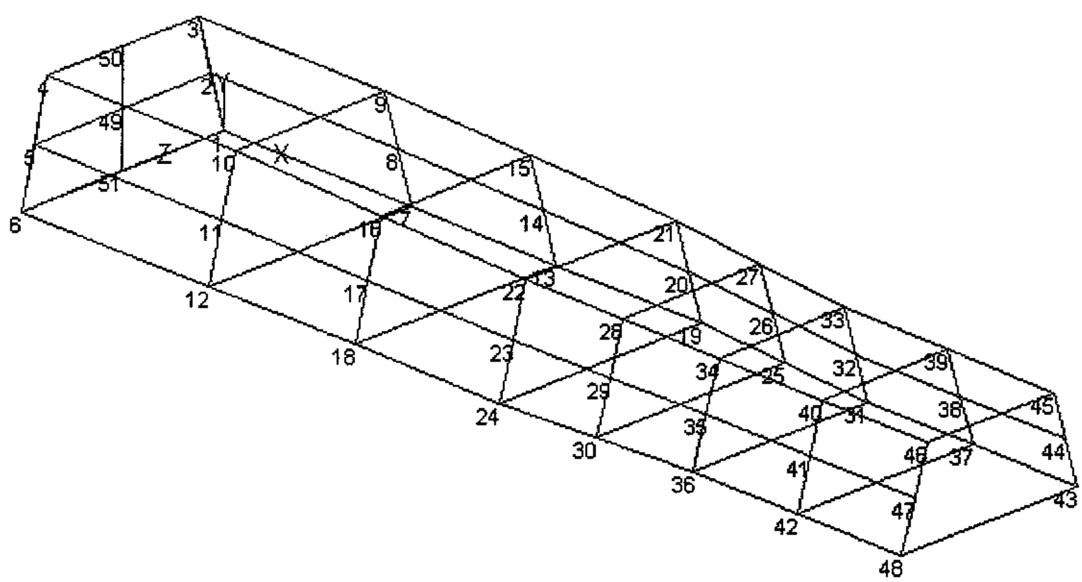

Figure 6 : Mesh of half a sleeper used in the modal analysis sofware.

2.2 Set-up

The equipment used during this experiment is the following and was set-up as in figure 7 :

- Hammer B&K type 8202/1271063
- 3 accelerometers B&K 4393
- 1 accelerometer B&K 4370
- 5 charge amplifiers B&K type 2635
- Analyser HP3566A/3567A.
- PC Elonex
- pieces of cork

Remarks :

✗ Different types of accelerometers were used because not enough of a single type were available.

✗ The PC is required to drive the analyser and to store the data.

✗ The pieces of cork provide a resilient foundation. The resonance frequency of the rigid body mode will be shown later to be about 22 Hz, which indicates that the foundation is soft enough. (The first bending mode occurs at about 120 Hz).

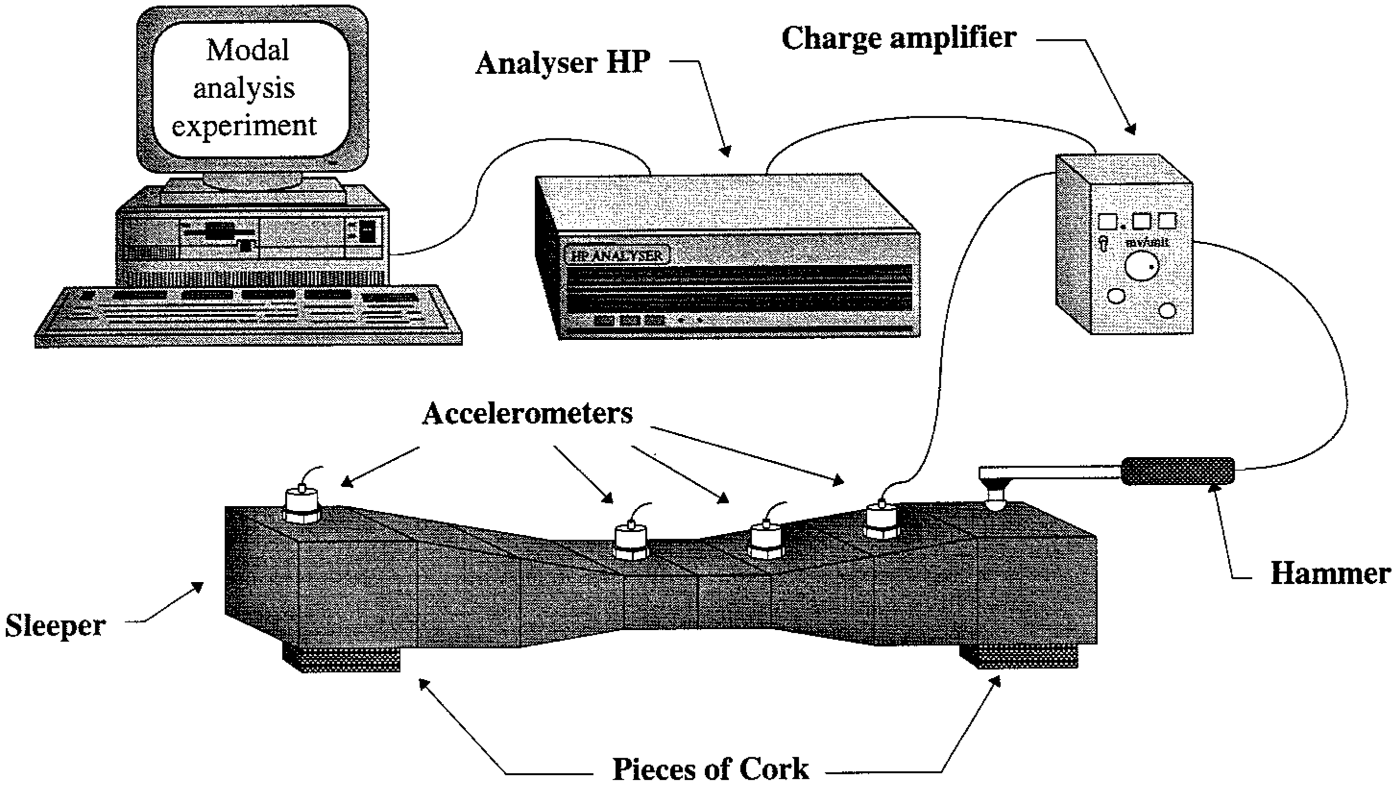

Figure 7 : Set-up of the modal analysis experiment

2.3 Experiment

To obtain the velocity distribution, normally the structure has to be excited at one or a few points and the velocity (or acceleration) measured on all the structure. Nevertheless, the principle of reciprocity says that the transfer function from a source at one point to a response at a second point is the same as the transfer function with the source and the response positions interchanged. Therefore, as the number of accelerometers is limited compare to the number of nodes of the sleeper mesh, it is very time-consuming to use the direct measurement, i.e. one fixed excitation and several responses. On the other hand, by using a hammer for the excitation, it is relatively easy to move this from one point to another. Therefore four nodes have been

been chosen to be response points where the transducers are fixed, and the rest of the nodes have been excited by the hammer.

Three different hammer tips are available for the hammer (steel, stiff rubber and soft rubber). In order to have good results, it is essential to have a good input power within the frequency range of the analysis. Therefore, the input power of each tip was measured and recorded. See figure 8, 9 and 10. It occurred that the steel tip has the smallest decrease of power within the frequency range (0-3200 Hz) of the study. This has therefore been used.

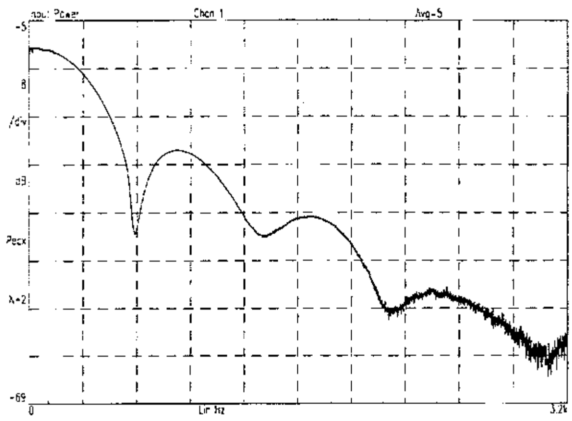

Figure 8 : Input power of soft rubber tip

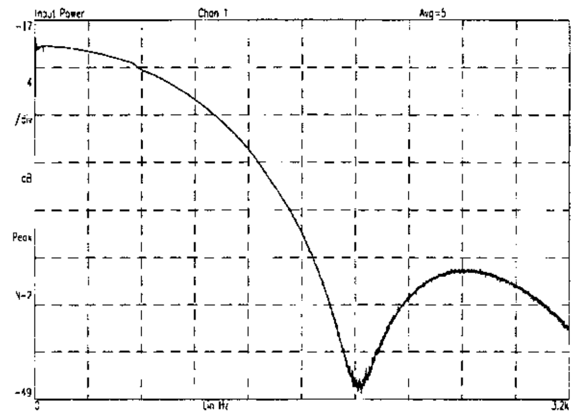

Figure 9 : Input power of stiff rubber tip

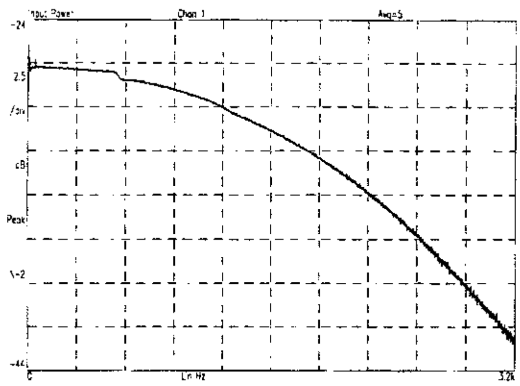

Figure 10 : Input power of steel tip

The first set of accelerometers was fixed at nodes 3, 16, 27 and 40, all four in the y-direction which is supposed to be the side which radiates the most. The hammer and the four transducers are each connected to one channel of the analyser. Then, for each excitation with the hammer at any node of the sleeper, the Frequency Response Functions (FRF) between the velocity of the response points and the force input were recorded (after an average of 5) thanks to the analyser. It has to be noted as well that a uniform window was used within a frequency range of 0-3200 Hz with a resolution of 3201 lines (i.e. one line per Hz).

The same experiment was carried out with a second set of accelerometers fixed now at nodes 4, 18, 28, 42 in the z-direction. Once again, the FRF were recorded with the analyser.

2.4 Results and modal analysis

2.4.1 Frequency response function and data processing

Figure 11 below shows the FRF (Frequency Response Function) of the node 4 (channel 2 of the analyser during the first measurement) when excited at node 9. As the number of FRF is about a hundred, only one typical graph is displayed in this report.

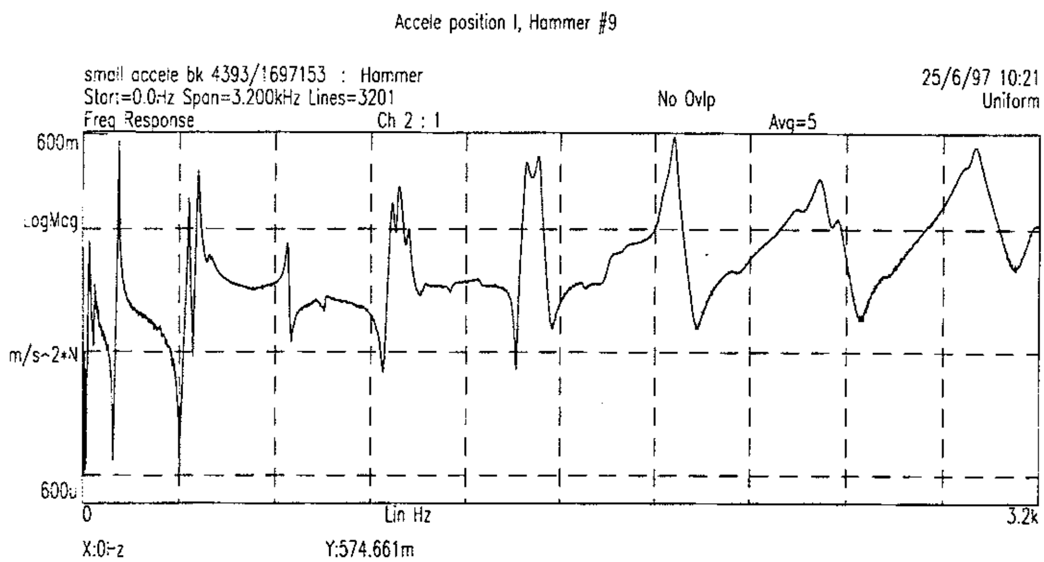

Figure 11 : Example of a Frequency Response Function

Firstly, before using the modal analysis software, the data files have to be transferred into files that can be read by the package. Each data file obtained during the measurement has to be transferred into MATLAB form and has to be divided into four different files for each of the frequency response functions (one for each of the four accelerometers used simultaneously)

For this, a software delivered with the analyser ("SDFTOML.exe") was used. The data files ".DAT" were separated into MATLAB format ".MAT" files representing the coherence, cross-spectrum, input power, output power and the frequency response functions (FRF). The latter were then imported into MATLAB and written to four separate text files using "DIARY" and were called ".FRH".

Each of these files represents the FRF of a particular response point to a particular excitation point. The velocity distribution of the sleeper can be determined from a combination of these files. The list of these files is given in Appendix B.

2.4.2 Modal analysis

After obtaining of the velocity distribution of the sleeper, it is possible to start the modal analysis within the software MODENT™ from ICATS. However, the software needs a lot of information within each of the FRF files, such as position of the excitation and the response, type of the FRF (in this case it is inertance), etc. Thus, each FRF files was edited to add the relevant information.

Once each file was compatible with the format required by the software, the modal analysis was carried out first on several single analyses, i.e. with only one FRF file. This first step of the analysis is useful to acquire a reasonable idea of the results. Then, a multiple analysis is processed within the software using several FRF files chosen at random among the 120 files. The number of files used in this analysis is 17 which allows the analysis to be quick and accurate. The results of this modal analysis are recorded below.

2.4.3 Results of modal analysis

The 17 FRF used within the modal analysis package are displayed in figure 12 and represents the inertance.

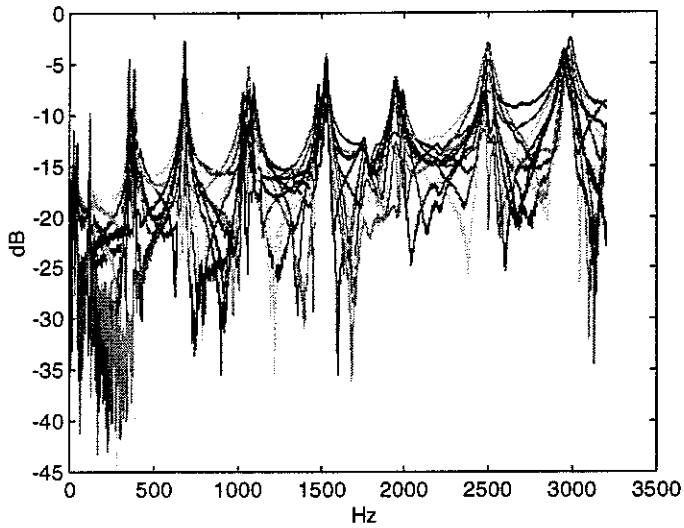

Figure 12 : The 17 FRF used in Modent

The natural frequencies and the damping loss factors of the mode of the sleeper are listed below in the Table 1 and 2.*

	Frequency in Hz	Damping
mode 1	21.5	11.04 %
mode 2	38.5	8.82 %
mode 3	119.6	0.79 %
mode 4	351.8	1.00 %
mode 5	382.6	1.42 %
mode 6	681.5	1.25 %
mode 7	1036.4	1.48 %
mode 8	1054.3	0.79 %
mode 9	1070.7	1.45 %

Table 1

	Frequency in Hz	Damping
mode 10	1090.1	1.62 %
mode 11	1482.5	1.09 %
mode 12	1526.7	1.04 %
mode 13	1943.0	2.02 %
mode 14	1984.7	0.88 %
mode 15	2488.7	2.00 %
mode 16	2496.4	1.59 %
mode 17	2951.2	1.76 %
mode 18	2986.2	1.28 %

Table 2

* See chapter 5 for comparison with results from another study by Vibratec.

3- REVERBERATION ROOM EXPERIMENT

3.1 Presentation of the experiment and theory.

3.1.1 Presentation

The second experiment took place in the reverberation room of the ISVR The aim of this experiment is to carry out a reciprocal measurement on the sleeper in order to obtain a relation between the radiated sound power and the force input to the sleeper : W/F^2.

3.1.2 Theory for reciprocal measurements

χ <u>Reciprocity relation:</u>

The principle of reciprocity defines an equivalence between two systems: it states that the output at point B due to an input at point A, is equal to the output at A if the equivalent input were applied at B. These input and outputs can have various forms, but for the current situation, the relevant systems are shown in figure 13.

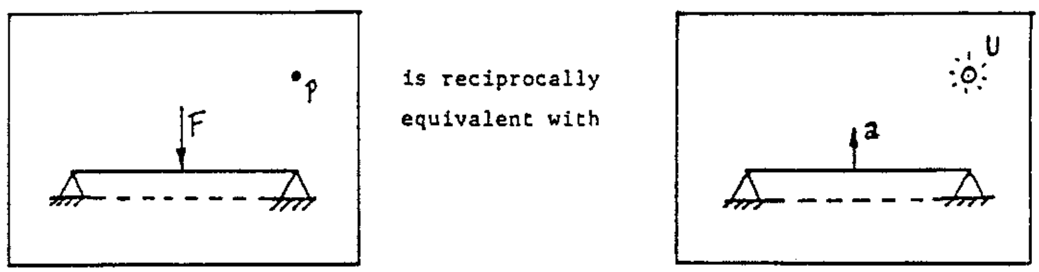

(a) Force F generates sound pressure p

(b) Sound source U generates structural acceleration a

Figure 13 : Relevant systems used for reciprocal measurement

In system 1, a sound pressure is generated at B, p_B, due to a force input on the structure at A, F_A, whereas in system 2, an acceleration is generated on the structure at A, a_A, due to a volume acceleration sound source at B,U_B. The reciprocity relation in this case is :

$$\frac{p_B}{F_A} = -\frac{a_A}{U_B} \tag{2}$$

Use of such a relation allows measurements of the transfer function from force to radiated sound to be made indirectly by measuring the acceleration on a structure due to a known external sound pressure. This has the advantage that a mechanical shaker does not need to be used, which thus avoids noise radiation by the shaker, as well as difficulties of introducing a force in a given direction.

✗ Sound power in a reverberation room

In order to apply this principle to measurement in a reverberation room, a relation is first required between an r.m.s sound pressure measurement, represented here by s, and the overall sound power, W, in the room. This is given as

$$W = s^2 \frac{13.82\ V}{\rho c^2 T_{60}} \tag{3}$$

where V is the volume of the room, T_{60} is the (frequency dependent) reverberation time (i.e. the time taken for a signal to decay to -60 dB of its level), ρ is the density of air, and c is the speed of sound in air.

It is assumed here that the sound pressure level has a uniform distribution through the room, which is true for a sufficiently high acoustic modal density. In practice, it would be measured as an average over a number of locations, or more practically by spatially averaging using a revolving microphone (on a boom).

χ <u>Sound pressure in a reverberant room due to a source U</u>

A volume acceleration source of r.m.s. amplitude U, generates a sound power given by

$$W = U^2 \frac{\rho}{4\pi c} \tag{4}$$

From equation (3) this means that, for a reverberant room, the source can be related to the r.m.s. sound pressure, which will now be given by p:

$$U^2 = p^2 \frac{13.82\ V\ 4\pi}{\rho^2 c T_{60}} \tag{5}$$

It should be noted that this relation is independent of the position of the source U, as well as the position of the sound pressure measurement.

χ <u>Reciprocal relation for the reverberant room</u>

Finally these equations can be assembled to give a relation between a measurable quantity: the ratios of the acceleration on the sleeper to the sound pressure in the room (excited externally by an arbitrary source U), and the desired quantity: the ratio of radiated sound power to a force input to the sleeper. From equation (3) :

$$\frac{W}{F^2} = \frac{s^2}{F^2} \frac{13.82\ V}{\rho c^2 T_{60}} \tag{6}$$

$$= \frac{a^2}{U^2} \frac{13.82\ V}{\rho c^2\ T_{60}} \tag{7}$$

$$= \frac{a^2}{p^2} \frac{13.82\ V}{\rho c^2\ T_{60}} \frac{\rho^2 c\ T_{60}}{13.82\ V\ 4\pi} \tag{8}$$

$$= \frac{a^2}{p^2} \frac{\rho}{4\pi c} = 0.08\ \frac{\rho}{c} \frac{a^2}{p^2} \tag{9}$$

Taking $\rho = 1.21$ Kg/m^3, and c = 340 m/s, this can be expressed in terms of decibels, as

$$10\log\left(\frac{W/W_0}{F^2}\right) = 10\log\left(\frac{a^2}{p^2}\right) + 84.5 \quad \textbf{(10)}$$

where $W_0 = 10^{-12}$ Watt so that the result is in dB re 10^{-12} Watt/N^2.

3.2 Set-up

The instrumentation used during the experiment is as follows :

- Accelerometer B&K 4378/1187979 of sensitivity 31.7 pC/ms^{-2}.
- Charge amplifier B&K type 2635.
- Microphone B&K 4133/873080.
- Preamplifier B&K type
- Rotating boom B&K type 3923.
- Measuring amplifier B&K type 2609 20-20000 Hz.
- Oscilloscope OS306 Gould 20 MHz.
- Analyser HP3566A/3567A.
- Noise generator (module of the analyser).
- Power amplifier HP400 high performance dual.
- PC Elonex
- Two Lifters, one Clarke-strong arm and one Weber Hydraulik
- Loudspeaker

The set-up is as following (see figure 14).

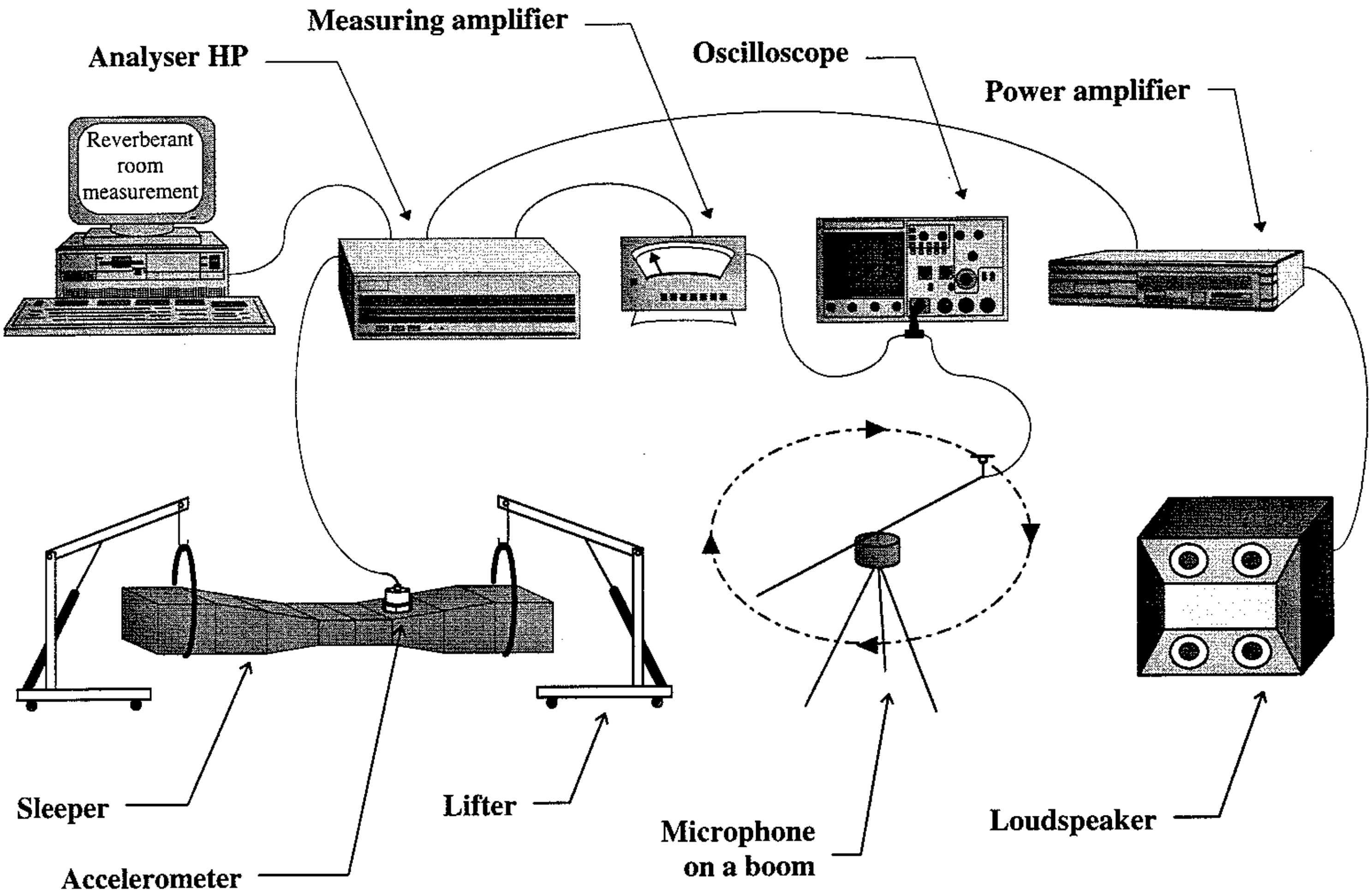

Figure 14 : Set-up of the reverberation chamber experiment

3.3 Experiment

Inside the reverberation room, the sleeper was lifted to around 1.5 metres from the floor to avoid the phenomena of standing waves underneath the structure. The room was excited by a white noise from a loudspeaker, placed in a corner of the chamber facing the walls, to generate a uniform distribution of the sound pressure level inside the reverberant room. The white noise was generated by the noise generator module of the analyser via a power amplifier. From the microphone on the rotating boom, the power spectrum of the pressure p^2 inside the chamber was time-space averaged during the measurement. The power spectrum of the acceleration a^2 of the sleeper was measured using a sensitive transducer. Several measurements were carried out for different positions of the transducer on the sleeper. Both of the power spectrum were recorded with the analyser.

3.4 Calibration

The results were stored for the first experiment in different files. The same processing as in section 2 was applied to these files to transfer them into MATLAB format and separate the different channels of the analyser. Then the calibration can be processed in MATLAB software.

The calibration of the power spectrum of the pressure inside the chamber was performed using a calibrator of 94 dB. The output voltage read on the measuring amplifier was recorded while the calibrator was on the microphone. It has to noted that the calibration must be done with the complete set-up identical to the one used during the real measurement.

χ Calibration of pressure:

$$94\text{dB} = 20\log\left(\frac{p}{p_0}\right) \quad \text{with } p_0 = 20 * 10^{-6} \text{ Pa}$$

$$\text{which gives} \quad ==> \quad p = 1.002374 \text{ Pa}$$

The output voltage during the calibration was V=13.5 mV which is related to the pressure p. Then, the pressure Pc related to a 1V output is :

$$Pc = p/V = 1.002374 / 0.0135 = 74.25 \text{ Pa/V}$$

Thus, to find the power spectrum of the pressure, the voltage has to be multiplied by Pc :

$$<p^2> = < v^2 * (74.25)^2 >$$

χ Calibration of acceleration:

The calibration of the power spectrum of the acceleration is related to the charge amplifier and the sensitivity of the transducer.

The sensitivity of the accelerometer is 31.7 pC/ms^{-2}. But as this sensitivity is too high to be set on the charge amplifier, the sensitivity was set at 3.17 pC/ms^{-2}. Therefore:

$$10 \text{ unit output } = 1 \text{ m/s}^2$$
$$1 \text{ unit output} = 0.1 \text{ m/s}^2$$

The gain on the charge amplifier was set at 1000mV/ unit output :

$$1000 \text{ mv} = 0.1 \text{ m/s}^2$$
$$1\text{V} = 0.1 \text{ m/s}^2$$

Thus, to find the power spectrum of the acceleration, the voltage has to be multiplied by 0.1 $m/s^2/V$

$$< a^2 > = < v^2 * 0.1^2 >$$

3.5 Results

The power spectrum of the acceleration and the pressure are displayed below on figure 14 and 15.

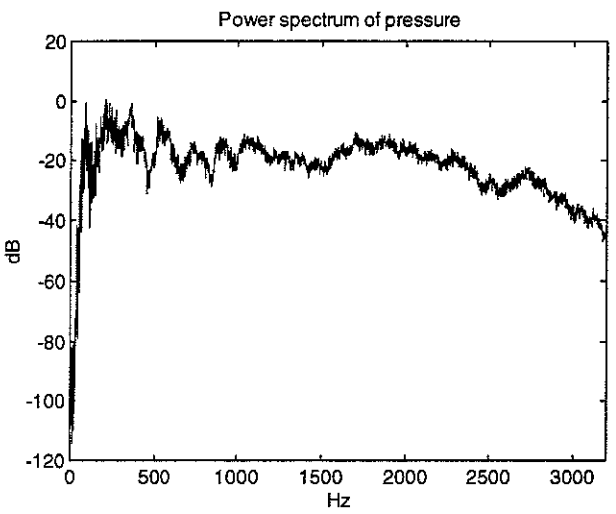

Figure 14

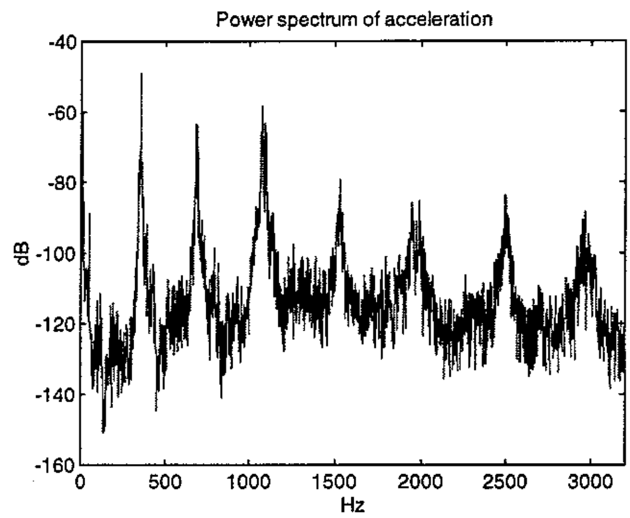

Figure 15

Then, knowing the power spectrum of the pressure and the acceleration, the relation between the radiated sound power and the force applied to the structure can be found using equation (9). Figure 16 shows W/F^2 in logarithmic scale (using equation (10)) with re dB = $1W/N^2$.

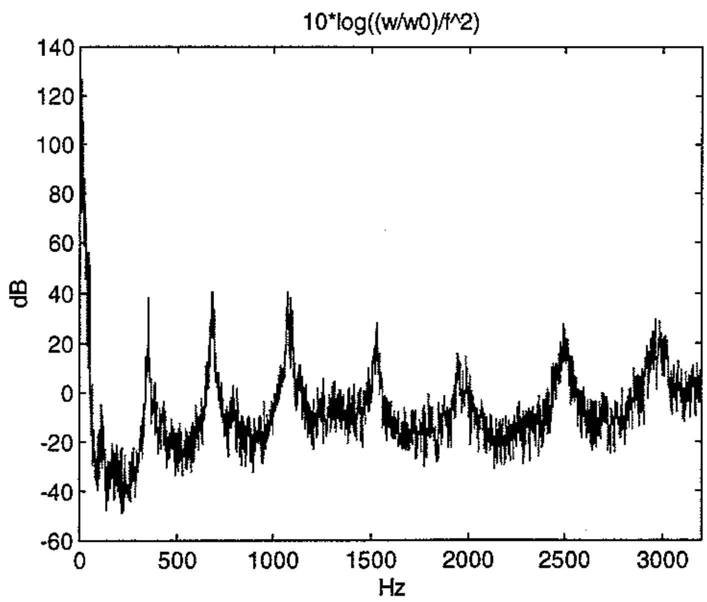

Figure 16

4- DATA PROCESSING AND RESULTS

4.1 Radiation efficiency

The radiation efficiency of the sleeper will be calculated by the following formula :

$$\sigma = \frac{W}{\rho c S < v^2 >} = \frac{W}{F^2} \Big/ \rho c \sum_i \frac{v_i^{\ 2}}{F^2} dS_i \qquad \textbf{(11)}$$

where W/F^2 was obtained in the reverberant room and the second part of the formula contains the velocity distribution of the sleeper obtained from the first experiment (hammer excitation) as following :

The velocity distribution acquired after the hammer measurement is in fact the distribution of the inertance a/F. Therefore, in order to find the radiation efficiency, it has to be processed into v^2/F^2, which is done using the following formula :

$$\frac{v^2}{F^2} = \frac{a^2}{F^2} \Big/ \omega^2 = \frac{a^2}{4\pi^2 f^2 F^2} \qquad \textbf{(12)}$$

However, the goal is to calculate the radiation efficiency at each mode of the structure. To do so, both the sound power and velocity distribution are integrated over frequency close to each mode. The results is as follows :

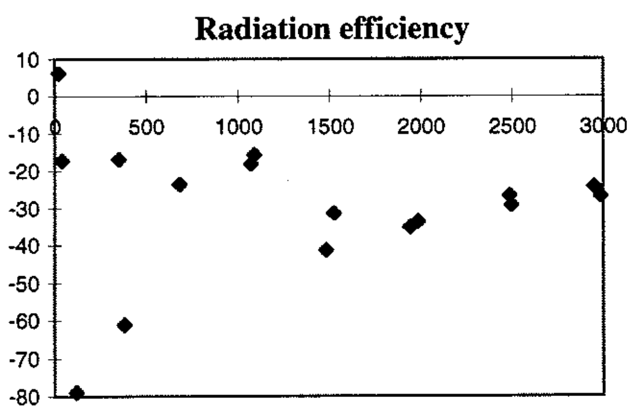

Figure 18

4.2 Mode shape

The following mode shapes were obtained. The fundamental mode (≈ 22 Hz) shown is a rigid body mode of the sleeper on the cork supports. The other modes are primarily flexural bending along the length of the sleeper.

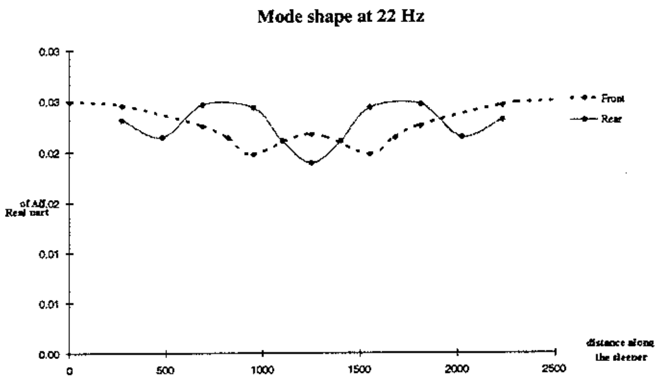

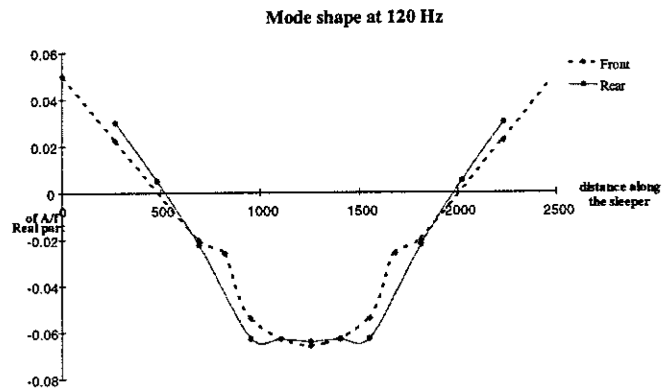

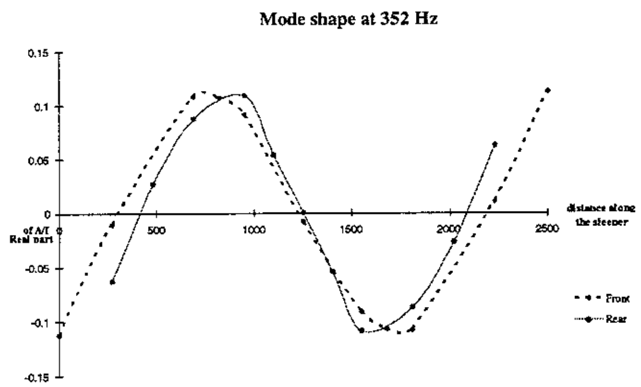

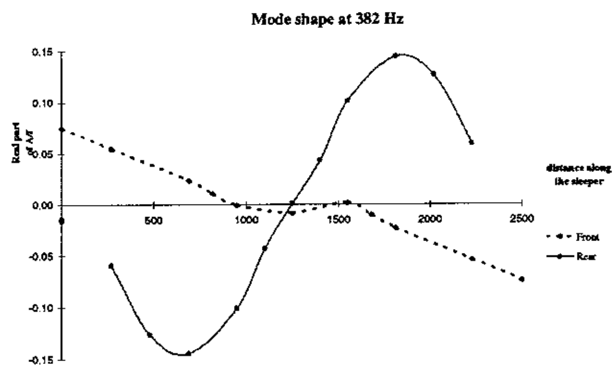

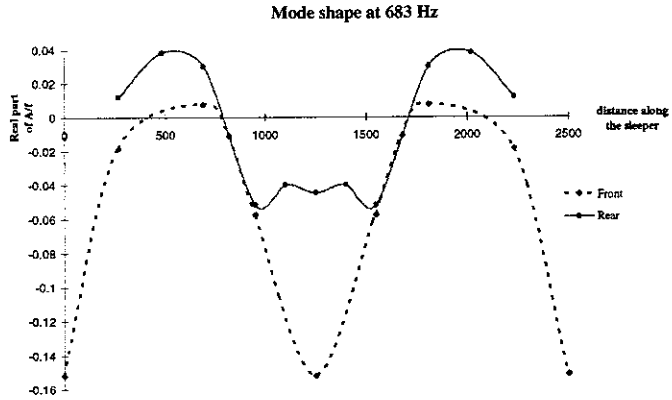

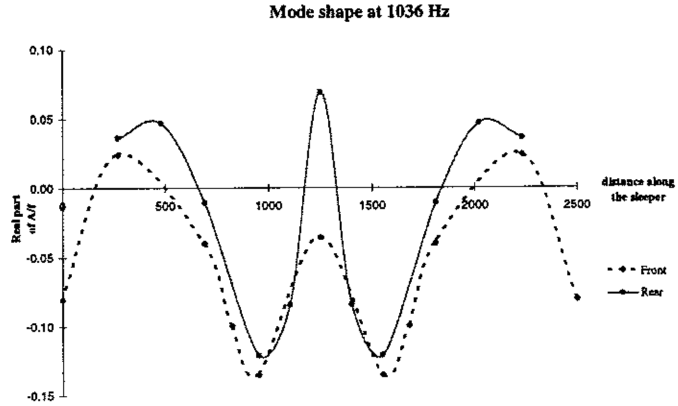

Mode shape at 1482 Hz

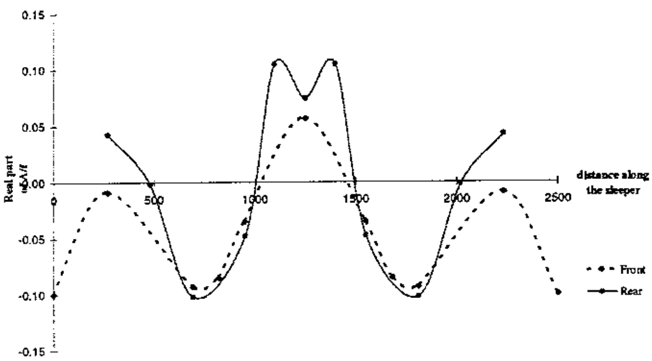

Mode shape at 1527 Hz

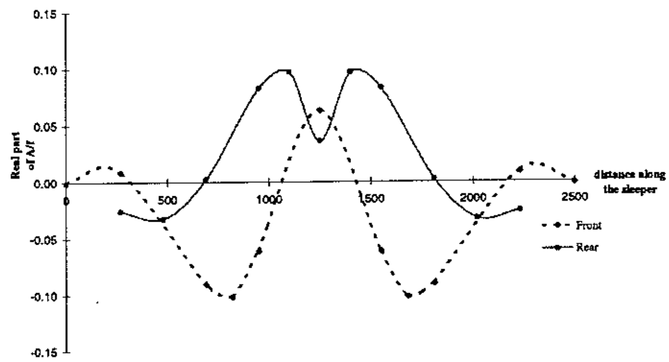

Mode shape at 1940 Hz

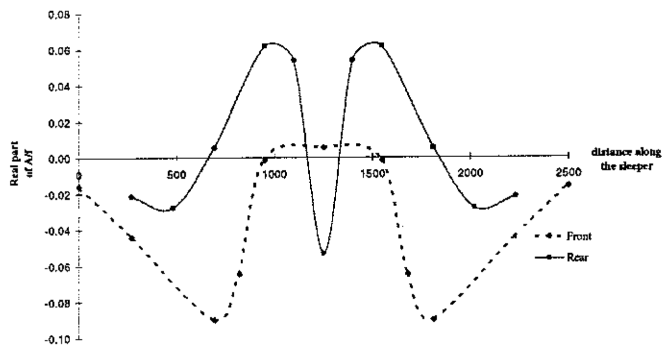

Mode shape at 1984 Hz

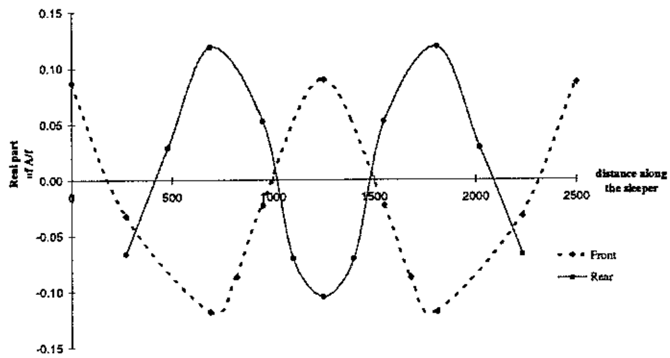

Mode shape at 2496 Hz

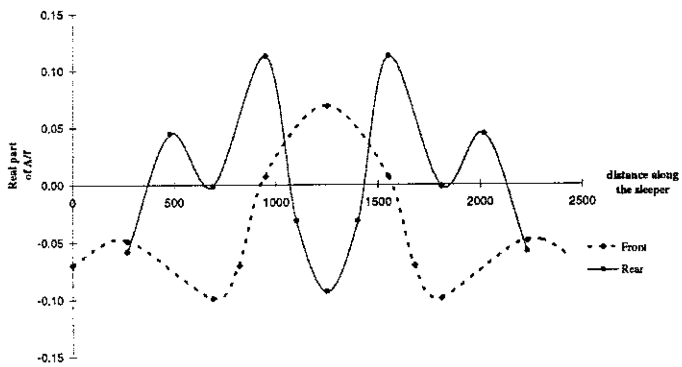

Mode shape at 2951 Hz

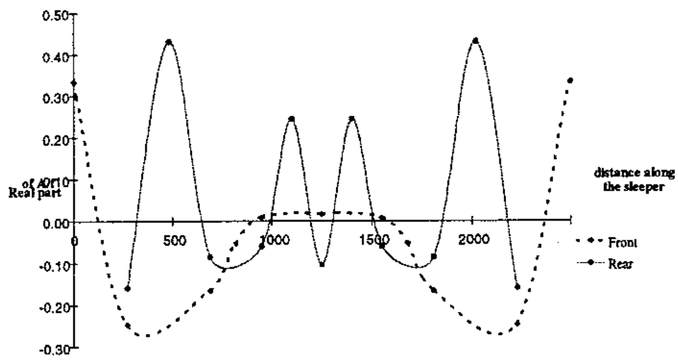

5- DISCUSSION

5.1 Comparison of natural frequencies

In the reference [16], Vibratec has carried out an experimental modal analysis on a monobloc concrete free sleeper type B 70-W. The results found in this project on a free reinforced concrete sleeper are recalled from chapter 2 in table 1 and 2. For comparison, the results of Vibratec are displayed in table 3.

	Frequency (Hz)	Damping in %
mode 1	21.5	11.04
mode 2	38.5	8.82
mode 3	119.6	0.79
mode 4	351.8	1.00
mode 5	382.6	1.42
mode 6	681.5	1.25
mode 7	1036.4	1.48
mode 8	1054.3	0.79
mode 9	1070.7	1.45

Table 1

	Frequency (Hz)	Damping in %
mode 10	1090.1	1.62
mode 11	1482.5	1.09
mode 12	1526.7	1.04
mode 13	1943.0	2.02
mode 14	1984.7	0.88
mode 15	2488.7	2.00
mode 16	2496.4	1.59
mode 17	2951.2	1.76
mode 18	2986.2	1.28

Table 2

	Frequency (Hz)	Damping in %
1st bending	112	0.9
2nd bending	340	1
3rd bending	652	1
4th bending	1026	1
5th bending	1450	0.8
6th bending	1909	0.9
7th bending	2389	0.8
8th bending	2891	0.8

Table 3 :Vibratec modal analysis results

Comparison between the results is reasonable if one considers modes 3, 4, 6, 7, 11, 13, 15 and 17 and the 8 bending modes of the Vibratec tested sleeper. The additional modes on the Tarmac sleeper could be the results of coupling with torsional modes of the sleeper. The variation of damping is wide in the result of this study but are probably not significantly different than the B 70-W sleeper.

5.2 Radiation efficiency

The final results of the radiation efficiency found in chapter 4, combining the results of chapter 2 and 3, appears quite unreasonable. Indeed, the radiation efficiency from any arbitrary structure, is assumed to converge towards unity (=0 dB) at high frequencies. However, the results, displayed in figure 18, show a radiation efficiency about -20 dB at high frequencies, which is unreasonable.

Also, it is still unclear whether this error comes from a calibration mistake (a non-calibrated hammer or an error in the microphone calibration) or whether it comes from the results of data processing error.

6- RECOMMENDED FURTHER WORK

Having obtained the radiation efficiency and the modal characteristics of the free sleeper, it is also important to check the effect on the noise radiation due to the fact that the sleepers, in real conditions, are in situ in the ballast.

It could then be possible to characterise the effect of the ballast on the sleeper (e.g. natural frequencies, mode shapes and damping as well as radiation efficiency) by comparing lab measurement on a free sleeper (that has been done during this project) and field experiment. This latter experiment is to be carried on a test track.

The installation of this railway track has been arranged by British Steel Track Products and installed by Grant Rail as subcontractors to British Steel for the ISVR at Chilworth.

The experiment to be carried out is an intensity measurement over the sleeper (uncoupled to the rail) and the ballast surrounding it, in order to get the sound power radiated from each item. The excitation of the structure would be an electrodynamic shaker (positioned near the rail footing) covered by an absorbent sealed box to reduce subsequently the extraneous noise transmitted through it. Also, it is important to obtain the velocity distribution of the sleeper in situ. This could be done by using acceleration transducers over the sleeper. Then, by integrating the intensity (see equation (13),

$$\frac{W}{F^2} = \int \frac{I}{F^2} ds \qquad \textbf{(13)}$$

the sound power radiated can be found and then combined with the velocity distribution to calculate the radiation efficiency of the sleeper in situ using equation (11) described in chapter 4 . From the sound power radiated from the sleeper and the ballast, it should also be possible to compare their contribution to the sound radiation over the frequency range.

Finally, the noise coming from the train measured in the field with microphones is partly reflected from the ballast. Scarce data about the absorption of the ballast is available. Therefore, it could also be interesting to study the ballast in terms of absorption or in terms of acoustic impedance. Additionally, the reflection could introduce a phase relationship between direct and reflected rays. The consequence of this relationship could also be investigated.

APPENDIX I

Coordinates of the nodes of the sleeper mesh .

nodes	X	Y	Z
1	0	0	0
2	0	112.5	18.75
3	0	225	37.5
4	0	225	252.5
5	0	112.5	271.5
6	0	0	290
7	270	0	0
8	270	112.5	18.75
9	270	225	37.5
10	270	225	252.5
11	270	112.5	271.5
12	270	0	290

nodes	X	Y	Z
13	480	0	0
14	480	107.5	18.75
15	480	215	37.5
16	480	215	252.5
17	480	107.5	271.5
18	480	0	290
19	690	0	0
20	690	102.5	18.75
21	690	205	37.5
22	690	205	252.5
23	690	102.5	271.5
24	690	0	290

nodes	X	Y	Z
25	820	0	10
26	820	97.5	28.125
27	820	195	46.125
28	820	195	243.75
29	820	97.5	261.87
30	820	0	280
31	950	0	20
32	950	92.5	37.5
33	950	185	55
34	950	185	235
35	950	92.5	252.5
36	950	0	270

nodes	X	Y	Z
37	1100	0	20
38	1100	92.5	37.5
39	1100	185	55
40	1100	185	235
41	1100	92.5	252.5
42	1100	0	270
43	1250	0	20
44	1250	92.5	37.5
45	1250	185	55
46	1250	185	235
47	1250	92.5	252.5
48	1250	0	270

APPENDIX II

- List of the frequency response function files used to find the radiation efficiency.

Format of file : Anm_r.frh

✗ where A means first experiment (i.e. position of accelerometer on the top of the sleeper)

✗ where n is the number of the node where the accelerometer is fixed

✗ where m is the excitation point (with hammer)

✗ and where r is the direction of excitation (1=x, 2=y, 3=z)

A164_2.frh	A1622_3.frh	A166_3.frh
A164_3.frh	A1624_3.frh	A169_2.frh
A1640_3.frh	A1628_2.frh	A1610_2.frh
A1642_3.frh	A1628_3.frh	A1610_3.frh
A1645_2.frh	A1630_3.frh	A1612_3.frh
A1646_3.frh	A1633_2.frh	A1615_2.frh
A1646_2.frh	A1634_2.frh	A1616_3.frh
A1648_3.frh	A1634_3.frh	A1618_3.frh
A1649_1.frh	A1636_3.frh	A1621_2.frh
A1652_2.frh	A1639_2.frh	A1622_2.frh

- File containing the power spectrum information (experiment in reverberant chamber) :

Pow16#2.mat

✗ where 16 is the position of the acceleration during the measurement in the room

✗ and where 2 is the direction of measurement of the acceleration (2=y)

REFERENCES :

1. D. J. THOMPSON, B. HEMSWORTH and N. VINCENT 1996 *Journal of Sound and Vibration* **193**(1), 123-135. Experimental validation of the twins prediction program for rolling noise . Part 1: Description of the model and method.

2. D.J. THOMPSON 1988 *Journal of Sound and Vibration* **120**(2), 275-280. Prediction of acoustic radiation from vibrating wheels and rails

3. D.J. THOMPSON 1991 *Procs Instn Mech Engrs* vol. **205**, *Part F* : *Journal of Rail and Rapid Transit.* Theoretical modelling of wheel-rail noise generation.

4. D.J. THOMPSON 1991 *Journal of Sound and Vibration* **161**(3), 421-446. Wheel-rail noise generation, part 3 : rail vibration

5. D. J. THOMPSON, P. FODIMAN and H. MAHE 1996 *Journal of Sound and Vibration* **193**(1), 137-147. Experimental validation of the TWINS prediction program for rolling noise, Part 2 : Results

6. D. J. THOMPSON 1996 *TNO report (TPD-HAG-RPT-93-0214).* TWINS theoretical manual, version 2.3. See chapter 6 : Sound radiation

7. M.H.A. JANSSENS and D. J. THOMPSON 1996 *TNO report (TPD-HAG-RPT-96-0108).* Improvement of ballast and sleeper description in TWINS. Step 2: Development and implementation of theoretical models.

8. P.J. REMINGTON 1987 *Journal of Acoustical Society of America* **81**, 1805-1823. Wheel/rail rolling noise, I: theoretical analysis

9. D.J. THOMPSON and N. VINCENT 1995 *Vehicle System Dynamics Supplement* **24**, 86-99. Track dynamic behaviour at high frequencies. Part 1: Theoretical models and laboratory measurements.

10. S.L. GRASSIE, R.W. GREGORY, D. HARRISON and K.L. JOHNSON 1982 *Journal of Mechanical Engineering Science* **24**, 77-90. The dynamic response of the railway track to high frequency vertical excitation.

11. N. VINCENT and D.J. THOMPSON 1995 *Vehicle System Dynamics Supplement* **24**, 100- 114. Track dynamic behaviour at high frequencies. Part 2: Experimental results and comparisons with theory.

12. S.L. GRASSIE 1993 *Journal of Sound and Vibration* **187**(5), 799-813. Dynamic modelling of concrete railway sleepers.

13. J. M. MASON and F. J. FAHY 1990 *Noise Control Engineering Journal* **34**, 43-52. Development of a reciprocity technique for the prediction of propeller noise transmission trough aircraft fuselages.

14. J. ZHENG, F. J. FAHY and D. ANDERTON 1994 *Applied Acoustics* **42**, 333-346. Application of a vibro-acoustic reciprocity technique to prediction of sound radiated by a motored IC engine

15. D. G. MACMARTIN, G. L. BASSO and F. W. SLINGERLAND 1995 *Journal of Sound and Vibration* **187**(3), 467-483. Aircraft fuselage noise transmission measurement using a reciprocity technique.

16. N. FREMONT, J. P. GOUDARD and N. VINCENT 1996 *VIBRATEC report ref. 072.028a.* Improvement of ballast and sleeper description in twins. Step1: experimental characterization of ballast properties. See Chapter 4.3.2 : Experimental modal analysis.